









U-Th-Pb Shrimp dating of hydrothermal monazite from the Trairão Gold Deposit – Alta Floresta Gold Province (Amazon Craton)

Mara Luiza Barros Pita Rocha^{1,2*} , Farid Chemale Junior^{1,3} , João Orestes Schneider Santos⁴ , Marcia Aparecida de Sant'Ana Barros² , Francisco Egídio Cavalcante Pinho² , Neal Jesse McNaughton⁵ , Paulo César Corrêa da Costa² , Malcolm Roberts⁶ 

Abstract

Alta Floresta Gold Province occurs in the center-south portion of the Amazon Craton. Trairão gold deposit, which is located in the Alta Floresta Gold Province, is hosted by 1878 to 1854 Ma arc-related granites. Two important Au deposits take place in the region, the Trairão and Chumbo Grosso, which are structurally controlled by N80°W/S80°E trending lineament and associated with quartz veins and disseminated sulfides in a strong phyllic alteration zone of the host granite. Hydrothermal monazite grains formed during the Au mineralization event occur as fine anhedral crystals filling fractures or as isolated grains associated with Ag, Au, molybdenite, barite, pyrite, galena, and sphalerite. The hydrothermal monazite grains contain very low U, relatively low Th, and moderate Nd and La contents. SHRIMP U-Th-Pb dating of these crystals yielded an age of 1798 ± 12 Ma for Trairão and 1805 ± 22 Ma for Chumbo Grosso Au-deposits, whereas magmatic zircon grains of the granitic host rocks yielded an age of 1854 ± 8 Ma. The ages obtained in this paper are similar to those reported by Assis (2015), who studied Pé Quente (Re-Os in molybdenite, 1792 ± 9 Ma and 1784 ± 11) and Francisco deposits (^{40}Ar - ^{39}Ar ages from sericitic halo: 1779 ± 6.2 and 1777 ± 6.3 Ma). Serrato *et al.* (2014) acquired Re-Os dating in pyrite and molybdenite from Juruena gold deposit. The results show isochronous ages at 1786 ± 1 Ma, with a model age at 1787 ± 3.2 Ma, suggesting a major Statherian gold metallogenic event at the Alta Floresta Gold Province region. Regional fluids-flow has a close relationship with the generation and concentration of several important economic deposits in the Eastern border of Alta Floresta Gold Province, including Pé Quente, Francisco, Juruena, Chumbo Grosso, and Trairão Au-deposits.

KEYWORDS: Hydrothermal monazite; U-Th-Pb SHRIMP dating; Au-bearing deposits; Alta Floresta Gold Province; Amazon Craton.

INTRODUCTION

The Amazon Craton (AC) was formerly considered a large Archean platform that underwent reworking and reactivation during the Proterozoic, with expressive anorogenic felsic magmatism (Amaral 1974, Almeida *et al.* 1981). Santos *et al.* (2004) recognized four domains within the Tapajós — Parima Province: Parima, Uaimiri, Tapajós, and Peixoto de Azevedo (Fig. 1). This study was carried out in the Southern Peixoto de Azevedo Domain, which is part of Alta Floresta Gold Province (AFGP).

The economic importance of Tapajós and Peixoto de Azevedo Domains motivated a regional mapping. In addition, exploration by mining companies resulted in thousands of surfaces and drill core samples for study (Santos *et al.* 2004).

Several gold and copper-gold deposits are found within the Proterozoic Tapajós and Peixoto de Azevedo domains, which are marked by successive magmatic arcs with steady-state and flare-up stages similarly to Sierra Nevada Batholith stages presented by Paterson and Ducea (2015).

The AFGP is composed of plutonic-volcanic sequences generated in magmatic environment arcs that have been developed and have been progressively added during the Paleoproterozoic Eon, which encompasses two distinct geochronology provinces: Tapajós — Parima and Rondônia — Juruena, according to Santos (2000) model. Historically, the AFGP has been an important gold-producing region in Brazil. It is located in the Northern part of Mato Grosso State of Brazil. This province occurs as WNW/ESE extending for over 500 km and forms a trending belt where multiple felsic plutonic-volcanic arcs are present, including also metasedimentary and collisional units called Nova Monte Verde Complex (Souza *et al.* 2005). There are several magmatic rocks formed between 2030 and 1780 Ma in at least four main flare-up stages (main period of crustal growth) at 2030–2000 Ma (Cuiú — Cuiú Complex),

¹Programa de Pós-Graduação em Geologia, Universidade de Brasília – Brasília (DF), Brazil. E-mails: marapita1@yahoo.com.br, faridchemale@gmail.com

²Faculdade de Geociências, Universidade Federal do Mato Grosso – Cuiabá (MT), Brazil. E-mails: mapabarro@yahoo.com, aguapei@yahoo.com, pccorrea.costa@gmail.com

³Universidade do Vale do Rio dos Sinos – São Leopoldo (RS), Brazil.

⁴University of Western Australia – Perth, Australia. E-mail: orestes.santos@bigpond.com

⁵Curtin University – Perth, Australia. E-mail: mcnaughton@curtin.edu.au

⁶Centre for Microscopy, Characterization and Analyses, University of Western Australia – Perth, Australia. E-mail: malc.roberts@uwa.edu.au

*Corresponding author.



1960–1980 Ma (Creporizão Suite), and 1860–1880 Ma (Matupá Suite).

GEOLOGICAL SETTING

The AFGP (Dardene & Schobbenhaus 2001, Santos *et al.* 2004) or Juruena — Teles Pires Gold Province (Silva & Abram 2008) extends over 500 km NW-SE in the Southeast portion of the AC (Souza *et al.* 2005). The province consists of plutono-volcanic units that belong to two geochronological provinces: Tapajós — Parima (2.0–1.88 Ga) and Rondônia — Juruena (1.82–1.54 Ga) according to Santos (2003), or Ventuari — Tapajós and Rio Negro — Juruena according to Tassinari and Macambira (1999). These provinces were interpreted as products of successive arc accretion, which involved important addition of juvenile material, as well as reworking of older continental crust (Tassinari & Macambira 1999, Santos 2000).

The AFGP is composed mainly of high potassium calc-alkaline granites (ranging from granodiorites to alkaline-feldspar granite). Although not present in the Eastern segment of AFGP, the Bacaeri — Mogno and Cuiú — Cuiú Complexes characterize

important regional units because they correspond to the oldest rocks in this province. The Bacaeri — Mogno Complex has been interpreted by some authors as a piece of evidence of a suture zone (Duarte *et al.* 2015). This Complex is represented by fragments of iron formation associated with mafic rocks that occur strictly in the West portion of the AFGP. The oldest granites in the region can be denominated as Cuiú-Cuiú Complex (2.1–1.99 Ga), which is represented in the area by tonalitic to granitic gneisses (Souza *et al.* 2005, Santos *et al.* 2004). Several high-K granites are present in the area and include the:

- Nhandu Intrusive Suite (1.96 Ga) (Barros *et al.* 2015);
- Matupá Intrusive Suite (1.87 Ga) (Silva *et al.* 2014);
- Juruena Intrusive Suite (including Paranaíta, Cristalino, Apiacás Granite) (1.82–1.79 Ga);
- Teles Pires magmatism (1760 Ma) (Pinho *et al.* 2003, Barros *et al.* 2009).

The Nhandu Intrusive Suite corresponds to magnetite-biotite monzogranite and syenogranite, usually with enclaves of diorite to quartz-monzodiorite (Silva & Abram 2008). Geochemically, the suite has metaluminous to peraluminous

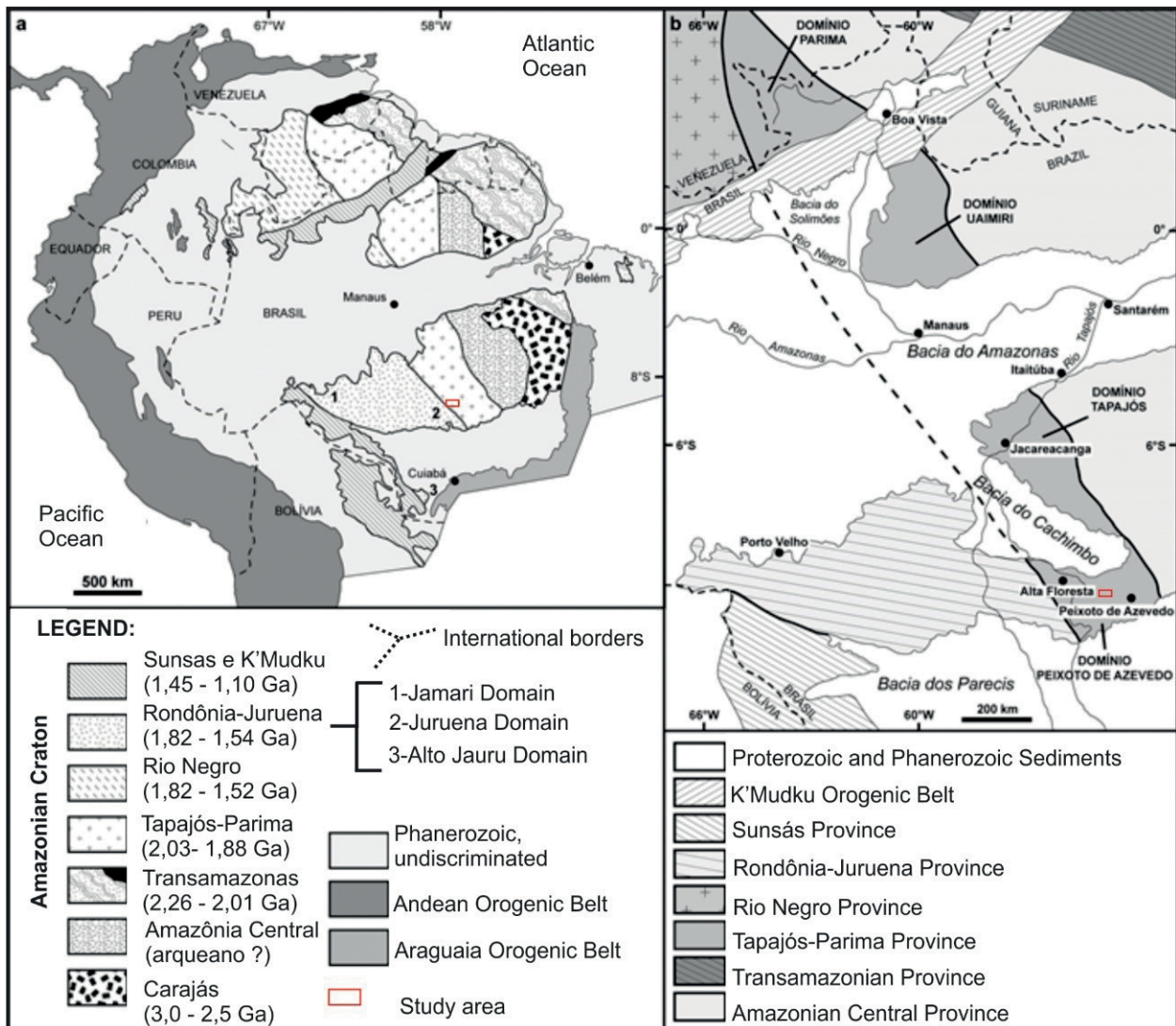


Figure 1. Maps with provinces age. (A) Map with Geotectonic Province model by Santos *et al.* (2003); (B) different metallogenic sub-domains of the Tapajós-Parima Orogenic belt (Santos *et al.* 2004).

patterns, with calcium-alkaline to subalkaline affinity, medium potassium and is FeO_t enriched (Souza *et al.* 2005). These rocks show a geochemical tendency of granites generated in magmatic arc to intra-plate environments (Paes de Barros 2007). Because this suite hosts primary gold mineralizations (Trairão Mines), it commonly shows evidence of potassic alterations with microcline formation accompanied by precipitation of sulfides and magnetite. The age of 1962 ± 7 Ma for the Nhandu Intrusive Suite was established in the outcrop by Barros *et al.* (2015) using U-Pb in zircon (SHRIMP).

The Matupá Intrusive Suite was originally named by Moura (1998) to highlight a body of isotropic biotite monzogranite, calcium alkaline with high potassium, and peraluminous to slightly metaluminous rocks. The Matupá granite in the Serrinha region (Moura 1998) crops out as undeformed and with small fractured blocks. A zircon Pb-Pb age of 1872 ± 12 Ma was obtained, with gold mineralization in quartz veins and porphyry type (disseminated and stockwork) that is associated with a major hydrothermal stage.

Silva *et al.* (2014) showed that a biotite monzogranite facies previously defined as belonging to Peixoto Granite (1790 Ma) is aged 1869 ± 10 Ma, similarly to the biotite monzogranites from Matupá Intrusive Suite.

The syenogranite that hosts the Trairão deposit presents hydrothermal style often represented by intense quartz shafting with formation of hydrothermal breccias and texture of the comb-texture type. Towards the mineralized zone, these venules become more abundant and develop a pervasive pattern that obliterates the primary structure of the host rock almost completely in some portions.

The main hydrothermal stage is represented by the large occurrence of quartz \pm pyrite \pm sericite in the environments of Trairão and Chumbo Grosso deposits. They occur mainly in the form of veins and hydraulic breccias with quartz matrix to which the ore is associated with. In the intensely hydrothermal portions, the pervasive alteration can be developed until complete replacement of the host rock. Silicification often forms stockwork type patterns in the form of interlaced veins of quartz \pm pyrite \pm sericite, and quartz vugs of medium to coarse granulation were also observed.

Characterization of the analyzed samples

Monazite grains were recognized with a scanning electron microscope (SEM). The analyzed samples are from outcrops and are often associated with barite, sphalerite, galena, and pyrite surrounded by a fine matrix characterized by sericitic alteration. Some tiny inclusions of scheelite, uraninite and more rarely inclusions of gold and silver were recognized by the SEM.

Titanite, magnetite, and more subordinately molybdenite were observed as accessory minerals associated with the mineralization from outcrops samples. The contact areas are characterized by intense silica injections in various directions, which strongly conditioned the porphyry contact zones. These areas are characterized by the development of dense stockwork systems, hydrothermal breccias cemented by quartz up to 3-m wide and preferred direction N82°E/S77°E, milky quartz veins and box-works sulfide, preferably pyrite and chalcopyrite.

Hydrothermal alteration and breccia type

The Trairão (TR-20 T) and Chumbo Grosso (TR-18 S) deposits are hosted preferentially by breccia veins in areas affected by hydrothermal alteration. Breccias are mainly poly-mictic and classified as magnetite-quartz and sericite breccia. These breccias contain angular to sub-rounded strongly altered fragments of granitic rocks and range from millimeters to few centimeters in diameter. The quartz fragments and wall rock (biotite syenogranite — Matupá Granite) are cemented by silica and alteration minerals. These breccias exhibit a fine-grained matrix of subhedral magnetite cemented by silica together with sulfides (pyrite, galena, chalcopyrite, sphalerite), monazite, barite, rarely uraninite and xenotime. Several comb veins crosscut the host, venules and/or pods filled with quartz \pm sulfides, which are common in this type of hydrothermal alteration, mainly in the Matupá Granite dome.

The post-magmatic sericitic alteration is evidenced by a sericite-dominated paragenesis that essentially substitutes the primary plagioclase. Accordingly, this alteration is well developed and represented by the paragenesis sericite \pm chlorite \pm calcite \pm hematite. On the other hand, chloritization also develops more locally in the altered rocks of both mines, which are represented by the chlorite \pm epitope \pm calcite mineral association. The hydrothermal breccia matrix has also been reported to include quartz grains surrounded by a sericitic matrix (Fig. 2).

Late stage venules of epidote and sulfides (pyrite and sphalerite) represent the later hydrothermal event system forming a hydrothermal style engulfing recrystallized quartz crystals. This mineral assemblage defines the hydrothermal Au-enriched zone in this granite. Pervasive secondary alteration (sericite + chlorite calcite + pyrite) is the most widespread hydrothermal alteration type in Chumbo Grosso deposit, and the occurrence of sulfites has been clearly associated with this alteration (Fig. 3).

In the silicified mineralized portions, which corresponds to the most important hydrothermal stage, there are cracks related to hydraulic contact areas with sub-volcanic granite, enabling percolation of hydrothermal fluids and probably the precipitation of sulfides. Based on field observations and petrographic analysis, the igneous textures suggest that the granite massif in question would be saturated in a fluid phase in shallow crustal levels (Candela 1997).

SEM analysis of mineralized sericite breccia samples have confirmed the presence of hydrothermal minerals, such as barite, pyrite, ilmenite and monazite, the latter usually included in sphalerite plus disseminated gold.

SAMPLING AND ANALYTICAL PROCEDURES

The SHRIMP II microprobe is able to analyze *in situ* grains as small as 10 microns. Thus, the dating of hydrothermal monazite by SHRIMP became widely used to determine the age of mineralization events (Lobato *et al.* 2007, Rasmussen *et al.* 2007, Martins *et al.* 2016).

Monazite grains were first observed in thin sections and then confirmed through the Energy Dispersive Spectroscopy (EDS)

using TESCAN-VEGA SEM at the Centre for Microscopy, Characterization and Microanalysis (CMCA) facilities of the University of Western Australia (UWA). Two samples were selected to search for hydrothermal monazite. They were collected in two pits of active mining named Trairão (TR20-T) and Chumbo Grosso (TR18-S). The sites where monazite grains were identified were marked at the surface of eight thin sections. Then, the sites were drilled using a micro-drilling device

(Dremel-2000) with bits of 3 and 5 mm in diameter. The resulting plugs were mounted in two epoxy discs of 25 mm in diameter (N15-12 and N15-13), metalized with carbon to take backscattered electrons (BSE) images in several magnifications to allow locating the grains during SHRIMP U-Pb analyses. The two mounts and a third mount carrying the monazite standards were cleaned and coated with gold for ion microprobe analyses. A total of 10 spots were analyzed in eight grains of monazite.

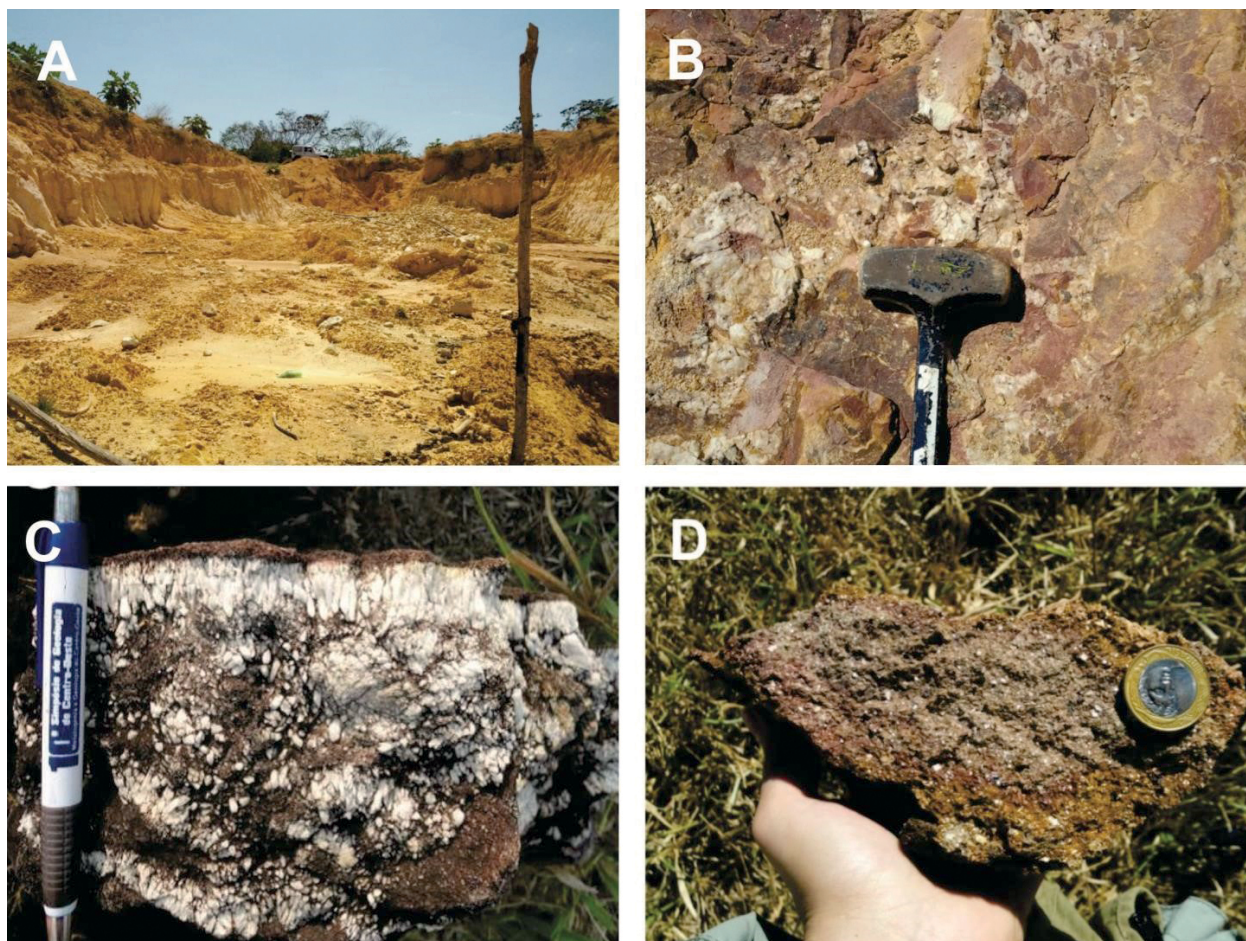


Figure 2. (A) Panoramic view of the artisanal mining in the Trairão region; (B) strongly altered biotite syenogranite crosscut by mineralized quartz veins and hydrothermal breccia; (C) comb structure quartz-vein; (D) detail of strongly altered biotite syenogranite from mineralized zone.

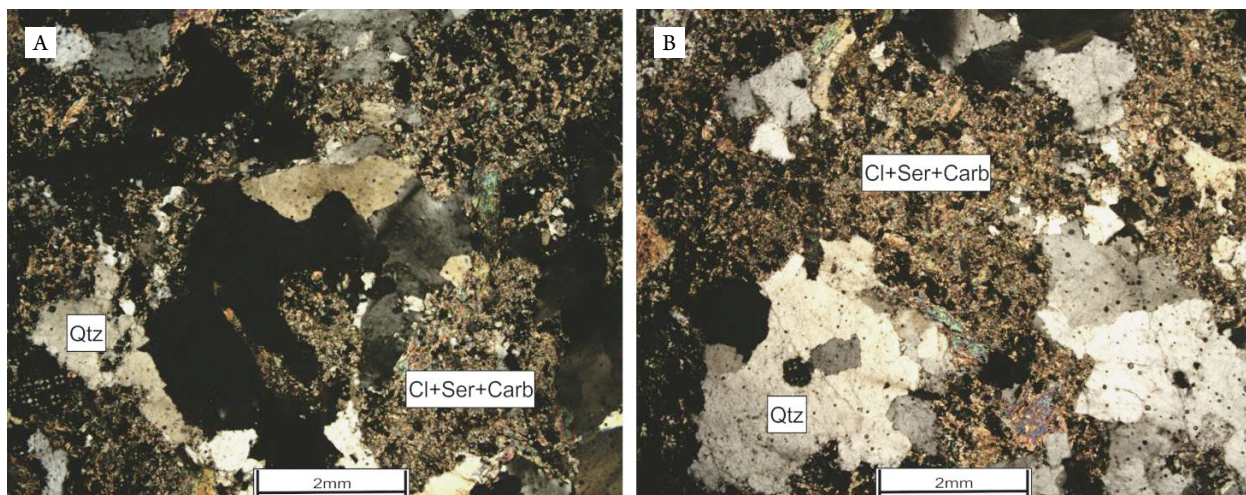


Figure 3. Photomicrograph of Chumbo Grosso deposit TR-18S showing: (A) quartz grains with irregular contacts dispersed in a matrix of pervasive sericite alteration; (B) pervasive sericite-chlorite-carbonate alteration obliterates the original texture of host biotite syenogranite, Matupá Suite Intrusive (crossed nicols).

U-Th-Pb isotope analyses of monazite were carried out on Sensitive High-Resolution Ion Microprobe II (SHRIMP II) B at Curtin University, Western Australia, following the procedures described by Compston *et al.* (1986) and Williams and Claesson (1987). Specific procedures to date monazite followed Stern and Sanborn (1998), including the use of retardation lens to suppress the background noise particularly around mass ^{204}Pb . The run table for monazite isotopic data acquisition is based on Foster *et al.* (2000), but it also included analyses of Nd and Y as suggested by Fletcher *et al.* (2010). The following sequence of 13 isotopic masses were analyzed: $^{202}\text{LaPO}_2$, $^{203}\text{CePO}_3$, ^{204}Pb , background, $^{205.9}\text{NdPO}_2$, ^{206}Pb , ^{207}Pb , ^{208}Pb , ^{232}Th , $^{244.8}\text{YCeO}$, ^{254}UO , $^{264}\text{ThO}_2$, and $^{270}\text{UO}_2$. Each analysis encompasses six or seven scans using a primary O^{-2} beam of about 0.6 nA. Standard Z2234 of 1026 Ma (Stern & Sanborn 1998) was used for the calibration of Pb/U ratio. Z2234 was selected for calibration because it is U-poor (200 ppm) and Th-poor (6,000 ppm). The available standard is more similar to the composition of the dated monazites. Additional analyzed standards are OX1 (511 Ma) and Z2908 (1796 Ma), the latter as a monitor for the $^{207}\text{Pb}/^{206}\text{Pb}$ ratio.

In situ U-Pb SHRIMP II zircon analyses were carried out in the hosting rock from two regions of Au mineralization in Trairão. Hand-picked zircons were mounted in an epoxy disc with chips of the TEMORA zircon standard, ground and polished, microphotographed in transmitted and reflected light and imaged using a SEM (BSE and charged contrast images). The mount was then cleaned and gold-coated in preparation for SHRIMP analysis. The used standard for calculation correction was the BR-266 with a $^{206}\text{Pb}/^{238}\text{U}$ age of 559 Ma.

Analytical and data reduction methods for monazite have been described by Rasmussen *et al.* (2001). Squid 2.5 software (Ludwig 2009) was used for reduction of data, whereas Isoplot 2.49 (Ludwig 2001) has been applied for construction

of concordia and mean average plots. All presented ages are calculated at 2 sigma or 95% confidence level using U decay constants from Jaffey *et al.* (1971).

Mineral chemistry

Compositional analyses were acquired on an electron microprobe (JEOL JXA8530F) equipped with five wavelength dispersive spectrometers. Operating conditions were 40 degrees takeoff angle and a beam energy of 20 keV. The beam current was 130 nA, and the beam diameter was fully focused. Elements were acquired using analyzed crystals LiF for Dy, Pr, Er, Nd, Gd, Sm, Yb, Eu, PETH for Th, Pb, PETJ for U, La, Y, Ce, Ca, P, PETH for Th, Pb, and TAP for Si.

The standards were crocoite for Pb; monazite for Th, Eu; Wollastonite for Ca, Si; uraninite for U; YPO_4 for P, Y; LaPO_4 for La; CePO_4 for Ce; PrPO_4 for Pr; NdPO_4 for Nd; SmPO_4 for Sm; GdPO_4 for Gd; DyPO_4 for Dy; ErPO_4 for Er; and YbPO_4 for Yb.

The counting time was 20 seconds for Pr, Nd, Gd, Sm, Yb, La, Ce, Ca, P, Eu; 40 seconds for Dy, Y, Er; 100 seconds for Si; and 200 seconds for Pb, Th, U.

The spell out background intensity data were calibrated and continuum absorption was corrected for U, Si, Pb, Th, Dy, Pr, Er, Nd, Gd, Sm, Yb, La, Y, Ce, Ca, P, and Eu. Unknown and standard intensities were corrected for deadtime.

Interference corrections were applied to U for interference by Th, Pr, Sm, Ce, to Si for interference by Nd, Er, to Pb for interference by Y, Th, to Th for interference by Gd, Y, to Dy for interference by Th, to Pr for interference by La, to Er for interference by Nd, to Nd for interference by Pb, Ce, Th, to Gd for interference by Nd, Ce, La, to Sm for interference by Ce, to Yb for interference by Dy, and to La for interference by Nd. Analytical results of the analyzed monazite are found in Table 1.

Table 1. Microprobe analysis of monazite grains from ore samples of Trairão (TR-20T) and Chumbo Grosso (TR-18S) gold deposits. All values are in %.

Sample/ Oxide	Chumbo Grosso Deposit						Trairão Deposit		
	TR-18S	TR-18S	TR-18S	TR-18S	TR-18S	TR-18S	TR-20T	TR-20T	TR-20T
	1 15-13A.1	1513A.2	1513A.3	15-3B.1	15-13B.2	15-13C.1	1512A.1	1512A.2	15-2A.3
CaO	0.16	0.11	0.21	0.32	0.33	0.26	0.22	0.2	0.31
Ce ₂ O ₃	29.7	32.23	32.52	31.15	30.82	31.18	31.26	31.52	30.58
Dy ₂ O ₃	0.68	0.3	0.22	0.52	0.45	0.35	0.57	0.44	0.47
Er ₂ O ₃	0.07	0	0	0.06	0.04	0	0.06	0.07	0.06
Gd ₂ O ₃	1.63	1.03	0.82	1.27	1.19	1.18	1.24	1.07	1.3
La ₂ O ₃	16.5	16.37	16.11	16.42	6.39	17.63	16.05	16.5	15.3
Nd ₂ O ₃	11.6	12.41	12.24	12.01	11.8	11.06	12.14	11.63	12.44
P ₂ O ₅	30.42	29.92	29.25	29.02	27.9	28.07	30	30.18	29.95
Pr ₂ O ₃	3.23	3.58	3.54	3.4	3.44	3.34	3.4	3.36	3.47
SiO ₂	0.07	0.14	0.32	0.15	0.26	0.92	0	0.08	0.04
Sm ₂ O ₃	2.26	1.88	1.76	1.93	1.83	1.8	1.95	1.68	1.98
Y ₂ O ₃	1.56	0.56	0.36	1.37	1	0.73	1.58	1.61	1.74
Yb ₂ O ₃	0	0	0	0	0	0	0	0	0
Sum	97.88	98.53	97.35	97.62	95.45	96.52	98.47	98.34	97.57

SHRIMP U-Th-Pb dating

U-Th-Pb isotope analyses of the selected monazite grains were carried out on the SHRIMP II at Curtin University of Technology following the procedures described by Compston *et al.* (1986), Williams and Claesson (1987) and Smith *et al.* (1998). After detailed photomicrography and BSE (backscattered) imaging, the mount was cleaned and coated with high-purity gold. BSE images were acquired at the CMCA. Monazite grains from two gold deposits, Trairão and Chumbo Grosso, were analyzed with ~ 0.5nA O₂ primary beam and 10 μm spots. Analytical and data reduction methods for monazite have been described by Rasmussen *et al.* (2001).

Ages were calculated using U decay constants from Jaffey *et al.* (1971). Analytical uncertainties given in Table 2 are shown in plots with 2 sigmas. Plots were prepared using ISOPLOT 2.49 (Ludwig 2001). After statistical analysis, the data were used in the construction of the concordia diagram.

RESULTS

Monazite grains selected from the magnetite-quartz and sericitic ore breccia matrix (Figs. 4 and 5) were analyzed to constrain the ore formation age and establish the time interval of the mineralizing events, respectively, for Trairão (TR20-T) and Chumbo Grosso gold (TR18-S) deposits. Figure 5B presents a monazite agglomerate, whereas in Figure 5D there is a monazite with three analyzed spots of ~10 μm.

The Rare Earth Element (REE) pattern normalized to chondrite (Nakamura 1974) (Fig. 6) shows a positive correlation between La, Ce, Eu and enrichment of LREE over some Heavy REE (HREE). The studied monazite grains are classified as Ce-monazites. This fact, combined with the morphology of monazite grains, tiny monazite grains, their chemical composition, besides the occurrence aggregated with minerals such as barite, pyrite, sphalerite and chalcopyrite (as shown in Fig. 4), supports the hypothesis that monazite is part of the

hydrothermal paragenesis and therefore suitable for dating the mineralization event (Poitrasson *et al.* 2000).

The mineralized breccia monazites also contain Y₂O₃ (0.4–1.7%), Pr₂O₃ (3.4%), Nd₂O₃ (11.1–12.4%) and Sm₂O₃ (1.7–2.3%), the positive correlation between these elements against P₂O₅ suggests a common metasomatic origin (Poitrasson *et al.* 2000) (Fig. 7). The analyzed monazites have total values between 95.45 and 98.53%, resulting most likely from non-analyzed elements such as Fe, F, Al and radiogenic Pb, or possibly meta-mictization processes occurring in monazite (Kucha 1980, Förster 1998).

However, studies show that in the case of monazite generated during hydrothermal activity, the chemical imbalance between U-Th-Pb, which is the product of fluid-mineral interaction, is minimal and occurs mainly along the fracture zones and mineral cleavage (Teufel & Heinrich 1997, Braun *et al.* 1998, Poitrasson *et al.* 2000). Thus, for chemical and SHRIMP II monazite analysis, we tried to avoid regions of the crystals with fractures and/or cavities (Figs. 5B-D).

Geochronology

Dates are presented as concordia ages, with probability of concordance plus evidence and associated mean square weighted deviation (MSWD). All the uncertainties of final ages are presented at 2-sigma confidence level. The results are presented in Figures 8 to 11, and supplemented by Tables 1, 2 and 3.

Samples from Trairão yielded a concordant age of 1798 ± 12 Ma, obtained from four individual analysis (Fig. 8). The remaining two analyses presented large errors and are discordant; therefore, they were not included for age calculations. The gold-bearing granite has been dated by U-Pb zircon, produced a concordia diagram age of 1854 ± 8 Ma, 18 zircon grains, as shown in Figure 10 (Rocha 2016).

Chumbo Grosso monazite grains are also concordant and yielded an age of 1805 ± 22 Ma, obtained from three spots points (Fig. 9). Granite rock that hosts this deposit has been

Table 2. U-Pb-Th SHRIMP isotopic data of monazites of Trairão and Chumbo Grosso gold deposits.

	Spot	U ppm	Th ppm	Th/U	Isotopic ratios										Ages					
					²⁰⁶ Pb ppm	²⁰⁸ Pb ppm	²⁰⁶ Pb* %	²⁰⁸ Pb* %	²⁰⁷ Pb / ²³⁵ U	error %	²⁰⁶ Pb / ²³⁸ U	error %	rho	²⁰⁶ Pb / ²³² Th	error %	²⁰⁶ Pb / ²³⁸ U	err 1s	²⁰⁷ Pb / ²⁰⁶ Pb	err 1s	disc. %
Trairão	12a.1-1	288	581	2.1	80	50	0.41	2.29	4.9446	2.29	0.3237	2.05	0.894	0.0966	1.57	1.808	32	1.812	19	0.3
	12a.1-2	847	2.288	2.8	245	198	0.08	0.23	5.0795	1.36	0.3367	1	0.734	0.0965	2.28	1.871	16	1.790	17	-5.2
	12a.1-3	1009	2.042	2.1	289	171	0.32	1.23	5.0124	1.67	0.3331	0.68	0.407	0.0937	2.19	1.853	11	1.785	28	-4.4
	12c.1-1	136	1.628	12.4	37	141	3.85	2.36	5.0478	7.89	0.317	1.3	0.164	0.0967	2.08	1.775	20	1.887	140	6.8
	12d.11	152	11.300	76.7	42	979	2.14	0.21	4.8701	3.6	0.3227	1.24	0.343	0.0967	2	1.803	19	1.790	62	-0.8
	12e.1-1	633	61.967	101.2	204	5.777	1.96	0.2	5.6855	4.39	0.3747	2.39	0.545	0.104	2.06	2.051	42	1.800	67	-16.3
Chumbo Grosso	13a.1-1	237	640	2.8	67	55	1.19	3.27	4.9882	2.24	0.3274	1.46	0.651	0.095	2.2	1.826	23	1.808	31	-1.1
	13a.2-1	33	3.177	100.9	9	278	7.71	0.59	3.939	16.41	0.3164	2.72	0.166	0.0976	2.02	1.772	42	1.432	309	-27.2
	13a.2-2	64	7.121	115.8	18	621	5.57	0.39	5.0856	9.54	0.3322	2.29	0.24	0.0974	2.01	1.849	37	1.817	168	-2
	13b.11	241	1.105	4.7	69	92	3.1	5.17	5.0958	3.01	0.3341	1.1	0.366	0.0933	2.17	1.858	18	1.810	51	-3.1
	13b.21	279	1.120	4.1	78	93	1.48	2.79	4.9302	2.52	0.3257	1.09	0.433	0.0928	2.17	1.817	17	1.796	41	-1.4

All Pb in ratios are radiogenic components, all corrected for ²⁰⁴Pb. Common lead (%) indicated by (*) calculated based on measured ²⁰⁴Pb. disc.: discordance, as 100-100{t[²⁰⁶Pb/²³⁸U]/t[²⁰⁷Pb/²⁰⁶Pb]}. Ratios in italic were not used for age calculations. rho: s (error correlation).

dated by U-Pb, magmatic zircon sample, and produced a concordia diagram age of 1878 ± 8 Ma (Fig. 11), with inherited zircons from 1923 Ma. Such inheritances are common in calcium-alkaline rocks from the AC. Both surrounding rocks are interpreted as belonging to the Matupá Intrusive Suite (Rocha 2016).

DISCUSSION

Monazites have been shown to be useful for dating magmatic and high-temperature metamorphic events (Parrish 1990), but this mineral can also be available for dating hydrothermal events, once proven its hydrothermal origin using quantitative electron microprobe analysis (EMPA). Usually, the EMPA allows the age determination of monazite crystals with high spatial resolution (up to $1 \mu\text{m}$ of crystal diameter), but the method is mostly used to date monazite with high amounts of Th and U (Montel *et al.* 1996, Cocherie *et al.* 2005). However, this method has some limitations to provide the precise age of hydrothermal monazite grains with low Th and U amounts,

in which the monazite crystals display complex, small-scale growth zoning. By using SHRIMP-II combined with detailed petrography and mineral chemistry, it is possible to determine an age of low-grade metamorphism or hydrothermal events with high precision *in situ* geochronology (*e.g.*, Ramussen *et al.* 2006). In the AC, there are reports from Souza *et al.* (2005b) of ages obtained from hydrothermal monazites in the Sn-bearing Bom Futuro at 997 ± 48 Ma.

The hydrothermal monazites from Trairão and Chumbo Grosso deposits are characterized as Ce-monazite. These results suggest that REE and phosphorus were mobile in hydrothermal fluids generated by metasomatic origin and monazites grew rapidly (Rasmussen *et al.* 2001). Morphological characteristics of monazite grains, mineral chemistry (slightly enriched contents of Ce) combined with U-Pb isotopes data, both from the mineralized zone and surrounding rock, suggest that monazites grew under hydrothermal fluids conditions related to a period of elevated thermal gradient during hydrothermal event, recording the age of the short-lived thermal event between 1878 and 1805 Ma. that took place during the

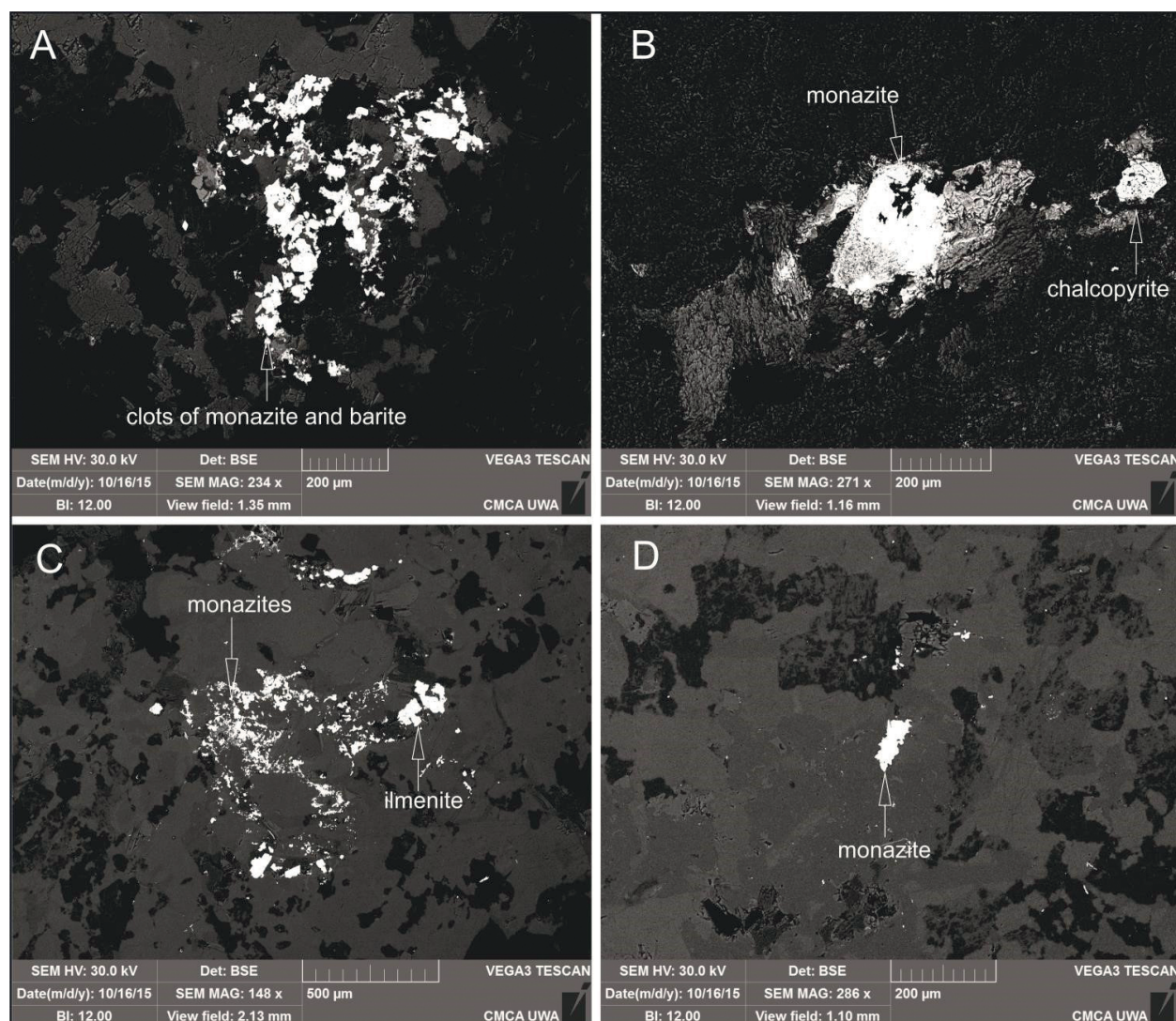


Figure 4. Representative backscattered electron images of thin section, sample TR-20T (Trairão) and TR-18S (Chumbo Grosso). (A) Clots of monazite grains associated with barite; (B) monazite grains showing apparent textural equilibrium with chalcopyrite; (C) monazite grains associated with ilmenite; (D) single monazite grain in the ore-bearing zone matrix.

Statherian period. This process was responsible for Au mineralization associated with granitic rocks at AFGP.

The monazites of Chumbo Grosso gold deposit have similar textural and chemical characteristics to those of the Trairão gold deposit, both containing lower Th and U contents (less than 1%), which are clearly different from typical magmatic and metamorphic monazite samples that usually present higher values for the same elements (Chang *et al.* 1996).

Samples of hydrothermal monazite (Trairão: TR-20T and Chumbo Grosso: TR-18S) from the matrices of magnetite-quartz and sericitic ore breccias (Fig. 3) yielded $^{206}\text{Pb}/^{238}\text{U}$ ages of 1798 ± 12 Ma and 1805 ± 22 Ma, respectively. We claim, based on mineralogical, geochemical and geochronological data presented herein, that hydrothermal monazites of the mineralized breccia, from Trairão and Chumbo Grosso deposits, indicate a hydrothermal deposit associated with the felsic magmatism in this sector of the AFGP.

The AFGP is a continental magmatic arc with several flare-ups (high volume of magmatism) and steady state (quiescence or low volume of magmatism) as presented by several

authors (e.g., Moura & Botelho 2002, Bettencourt *et al.* 2016). Several magmatic events are recognized by the occurrence of several Tapajônicos Magmatic Arcs (*sensu* Bettencourt *et al.* 2016) with the following geochronology: hydrothermal gold and gold-base metal deposits in the AFGP are structurally

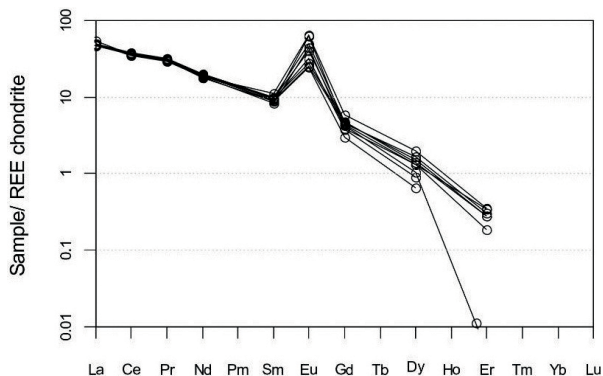


Figure 6. Representative rare earth element (REE) concentrations in monazite grains from ore breccia zones of the Trairão and Chumbo Grosso gold deposits. Chondrite values are from Nakamura (1974).

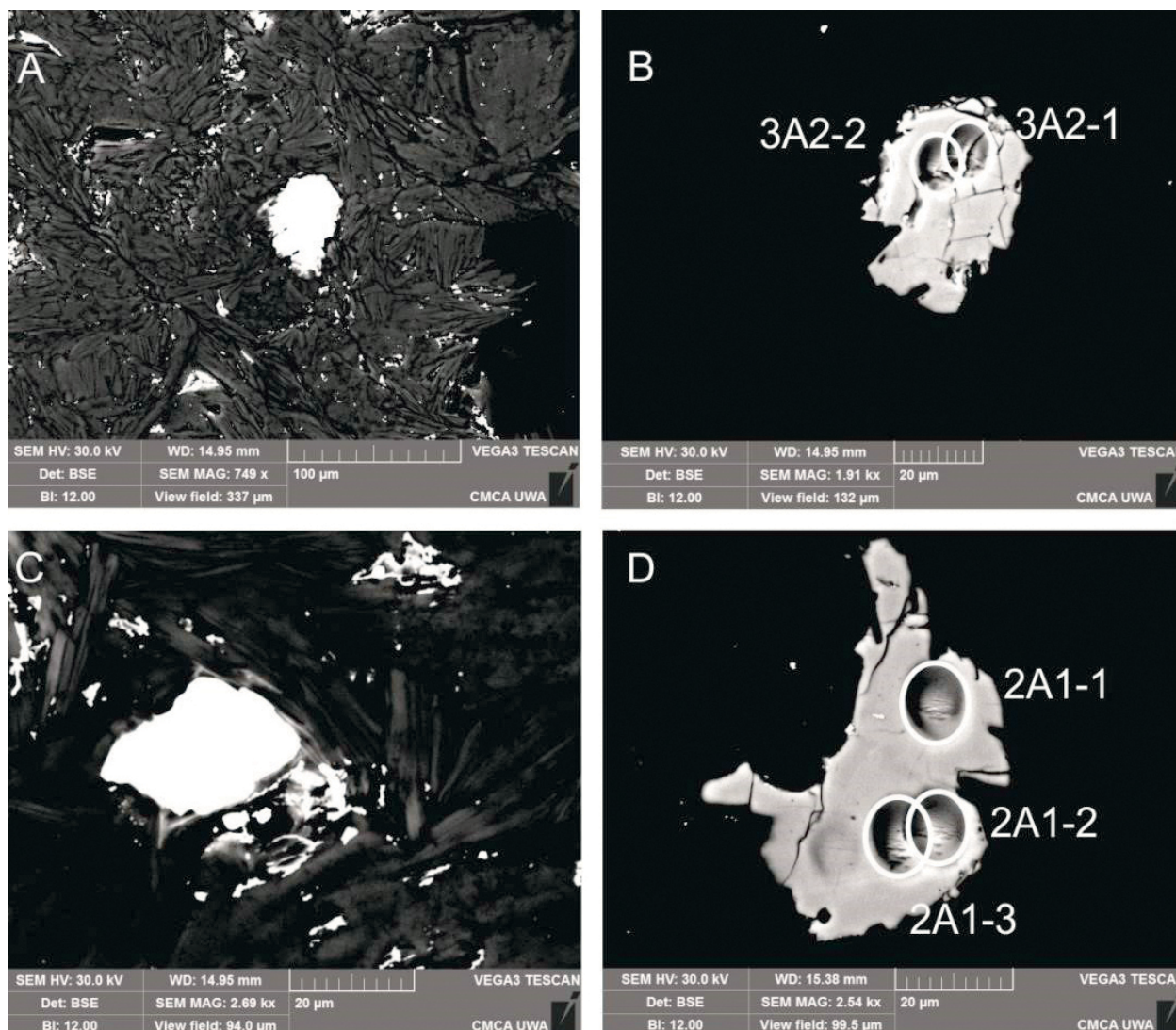


Figure 5. Scanning electron microscope backscattered electron (BSE) images of samples TR-20T and TR-18S: (A) detail of monazite grain from Chumbo Grosso deposit (TR-18S) with approximately 40 μm size, prior to the SHRIMP II analysis; (B) monazite grain from TR-18S showing two spot areas indicated by circles with approximately 10 μm in diameter; (C) detail of monazite grain from Trairão deposit (TR-20T) with approximately 30 μm size; (D) monazite grain from TR-20T showing SHRIMP II analytical spot areas add colon by circles with approximately 10 μm in diameter.

controlled and consist of quartz veins and hydrothermal breccias associated with the widespread magmatic activity. Knowledge fluid flow is important not only for economic studies, but also because it plays an essential role in the chemical and petrological evolution of the crustal crust (e.g., Ague 2014, Yardley 2009).

Based on Re-Os pyrite and molybdenite ages, Assis (2015) argues that an important gold metallogenic event took place in the Eastern sector of the AFGP, between 1.78 and 1.79 By. This event was responsible for the genesis of Luizão (1790 ± 9 Ma

and 1782 ± 9 Ma), Pé Quente (1792 ± 9 Ma to 1784 ± 11 Ma) and X1 (1787 ± 7 Ma to 1785 ± 7 Ma) intrusion-hosted disseminated gold deposits, whereas the same author working with the Francisco deposit, a gold-base metal similar to the Trairão deposit, showed that ⁴⁰Ar/³⁹Ar plateau ages from the sericitic alteration halo yielded ages from 1779 ± 6.6 Ma and 1777 ± 6.4 Ma. This author also concluded that the 1.78–1.79 Ga gold event may be temporally linked to the felsic magmatism of the Colíder (1.82–1.77 Ga), Paranaíta (1.81–1.79 Ga) and

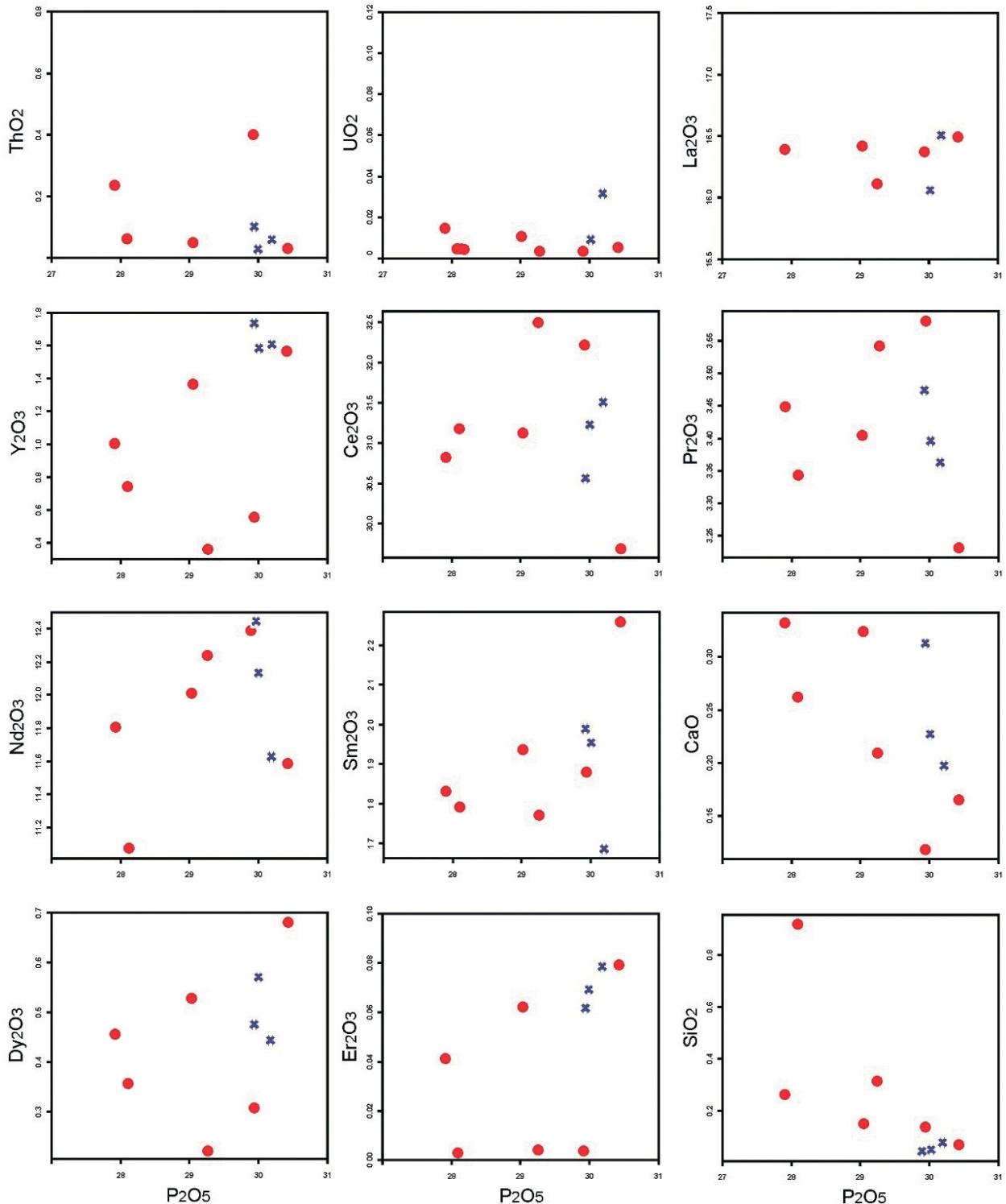


Figure 7. Bivariate diagrams for major and minor elements in monazite grains from ore breccia from Trairão (blue crosses) and Chumbo Grosso deposits (red circles).

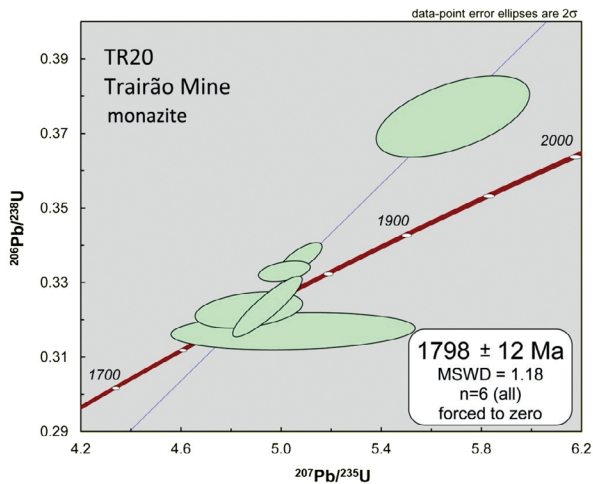


Figure 8. U-Pb Concordia diagram of SHRIMP II data for monazite from the Au-mineralized breccia in Trairão deposit (TR-20T). Inset shows 1798 ± 12 Ma, mean square weighted deviation (MSWD) = 1.18.

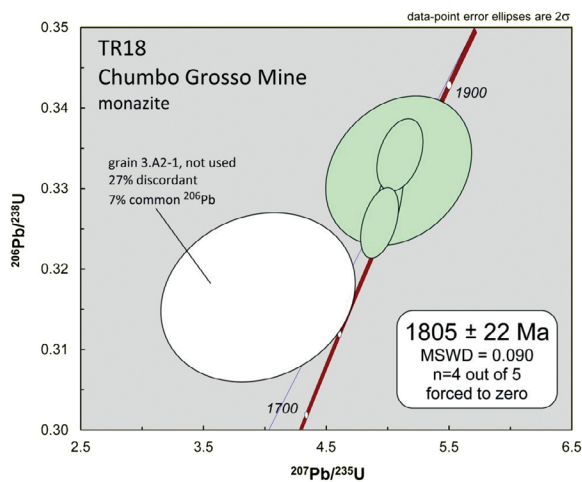


Figure 9. U-Pb Concordia diagram of SHRIMP II data for monazite from the Au-mineralized veins in Chumbo Grosso deposit (TR-18S). Inset shows 1805 ± 22 Ma, mean square weighted deviation (MSWD) = 0.090.

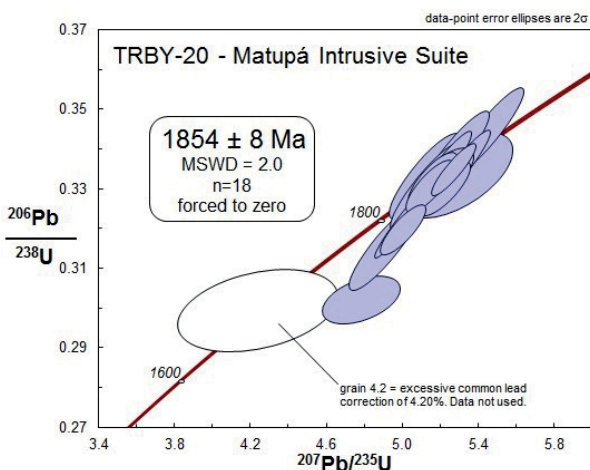


Figure 10. U-Pb Concordia diagram of SHRIMP II data for magmatic zircon sample TRBY-20. Inset shows 1854 ± 8 Ma (mean square weighted deviation — MSWD = 2.0) interpreted as the crystallization age of the host rock and as belonging to the Matupá Suite Intrusive (Rocha 2016).

Teles Pires (1.78–1.75 Ga) Suites, and that porphyry intrusions of 1.77 Ga, such as the one of the X1 and Francisco deposits, may have played an important role in the ore-forming processes.

The gold mineralization age obtained in the present study points to a mineralization age associated with the period of the Juruena magmatic arc activity (1.78–1.79 Ga), which was also related by Assis (2015), since the obtained monazite ages were dated at 1798–1805 Ga (Tab. 4).

The processes occurred by fluid percolation and mineral precipitation were evidenced by the presence of Au mineral deposits in mineralized hydrothermal breccias during 1.798–1.805 Ma. These data are also consistent with the Re-Os molybdenite model age of 1805 ± 7 Ma obtained by Acevedo (2014) for the Juruena gold deposit, AFGP northwestern sector. Considering the crystallization age of the Matupá Granite presented in this work, the host rocks of the gold mineralization between 1854 and 1878 Ma would indicate gold mineralization to be 73 to 55 million years younger than its host rock.

In this contribution, we present the mineral chemistry, coupled with U-Pb isotopes and petrographic determinations from quartz breccia associated with gold deposit, to investigate the timing responsible for this hydrothermal regional event that took place at the AFGP.

The results presented in this paper, together with an extensive data compilation, are used to compare the age obtained from hydrothermal minerals and corroborate with the hypothesis that there is a larger number of gold deposits in the AFGP that are related with the later magmatism of Tapajós-Parimá Province (Juruena Arc), which is responsible for remobilization and transport of gold-enriched hydrothermal fluids, during the Statherian period. This fluid flow activity lasted at least 10 million years, in Trairão and Chumbo Grosso deposits.

Recently, Gonçalves *et al.* (2019) delimited a time interval of approximately 20 million years of development for a widespread hydrothermal system in the Araçuaí Orogeny, using U/Pb ages of hydrothermal minerals (monazite, rutile, and xenotime).

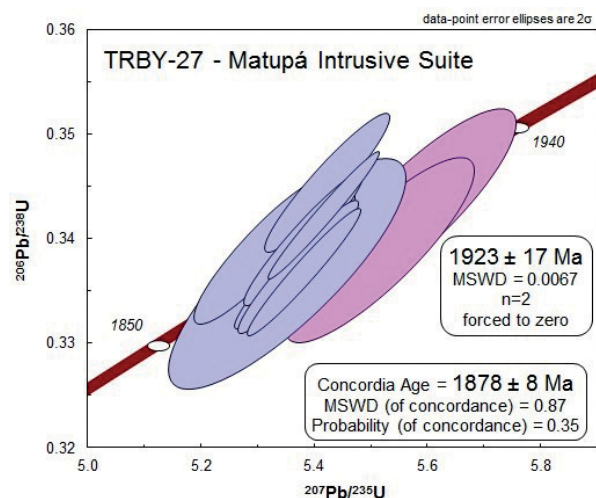


Figure 11. U-Pb Concordia diagram of SHRIMP II data for magmatic zircon sample TRBY-27. Inset shows 1878 ± 8 Ma interpreted as the crystallization age of the host rock, with inherited age of 1923 Ma, interpreted as belonging to the Matupá Suite Intrusive (mean square weighted deviation — MSWD = 0.87).

Therefore, regional fluid-flow has a close relationship with the generation/concentration of several important economic deposits in the São Francisco craton, including the Eastern Brazilian Pegmatite Province, Au-Pd-Pt deposits, and topaz deposit.

CONCLUSIONS

Gold mineralization in Trairão and Chumbo Grosso deposits in the Eastern sector of the AFGP are associated with breccias and quartz veins hosted mainly by a biotite syenogranite interpreted as part of the Matupá Intrusive Suite (1860 Ma), which evolved through the continental magmatic arc. The timing of fluid flow and implications for hydrothermal ore deposits across large parts of AFGP remains poorly understood.

These Au-bearing breccias exhibit a fine-grained matrix cemented by silica together with sulfides (pyrite, galena, chalcopyrite, sphalerite). Monazite, barite, rarely uraninite and xenotime, occur as accessory minerals. Our geochemical study of monazite revealed compositions enriched in light REE when compared to heavy RRE, with a positive anomaly of La, indicating a hydrothermal source.

The U-Th-Pb data in hydrothermal monazite yielded an age of 1798 ± 12 Ma (Trairão deposit) and 1805 ± 22 Ma (Chumbo Grosso deposit). This confirms that the mineralization is younger than the age of intrusion of the host rocks of Trairão (1854 ± 8 Ma) and Chumbo Grosso (1878 ± 8 Ma).

Many intrusions in the AFGP show the same age obtained for the hydrothermal monazite (Paranaíta Suite, Cristalino Granite, Guarantã Granite, and Juruena Intrusive Suite). This demonstrates a genetic relation between the emplacement of these plutons and the remobilization of hydrothermal fluids that were responsible for gold mineralization in large parts of the province.

The ages obtained in this paper are similar to those reported by Assis (2015), who studied the Pé Quente and Francisco deposits. In Pé Quente, Assis (2015) used Re-Os in molybdenite and found ages between 1792 ± 9 Ma and 1784 ± 11 Ma. In the Francisco Deposit, Assis (2015) applied ^{40}Ar - ^{39}Ar ages from sericitic halo, and the results were the same: 1779 ± 6.2 and 1777 ± 6.3 Ma. New Re-Os dating in pyrite and molybdenite acquired an isochronous age of 1786 ± 1 Ma, with a model age of 1787 ± 3.2 Ma, suggesting a major Statherian gold metallogenic

event in AFGP. This activity was developed for approximately 10 millions of years (Xavier *et al.* 2013, Assis 2015) and allowed those authors to correlate the ore-forming processes with the post-collisional felsic magmatism during the installation of the Juruena Arc (1.8–1.75 Ga), possibly chrono-correlated with the Colíder Group and Teles Pires Granites.

The results presented in this paper, together with an extensive data compilation, were used to compare the age obtained from hydrothermal minerals and corroborate with the hypothesis that there is a large number of gold deposits in the PAAF

Table 4. Compilation of U-Pb ages (LA-ICP-MS and SHRIMP), ^{40}Ar - ^{39}Ar of hydrothermal alteration and Re-Os in sulfide of host rocks and deposits investigated in the Eastern sector of AFGP.

Deposit	Ages	Method
Pé Quente (1) (3)	1.792 ± 9 Ma	Re-Os
	1.784 ± 11 Ma	(pyrite and molybdenite)
Luizão Deposit (1)	1.790 ± 9 Ma	Re-Os
	1.782 ± 9 Ma	(pyrite and molybdenite)
X1 (1)	1.787 ± 7 Ma	Re-Os
	1.785 ± 7 Ma	(pyrite and molybdenite)
Pé Quente (2)	1.833 ± 6 Ma	$^{40}\text{Ar}/^{39}\text{Ar}$ -muscovite
	1.830 ± 4 Ma	(hydrothermal alteration)
Francisco (2)	1.779 ± 6 Ma	$^{40}\text{Ar}/^{39}\text{Ar}$ -muscovite
	1.777 ± 6 Ma	(hydrothermal alteration)
X1 (2)	1.733 ± 6 Ma	$^{40}\text{Ar}/^{39}\text{Ar}$ -muscovite
	1.751 ± 6 Ma	(hydrothermal alteration)
Trairão (TR-20T) (4)	1.808 ± 19 Ma	SHRIMP
	1.766 ± 30 Ma	$^{207}\text{Pb}/^{206}\text{Pb}$ -monazite
Juruena Gold Deposit (5)	1.794 ± 29 Ma	(hydrothermal alteration)
	1805 ± 7 Ma	Re-Os (molybdenite)
Chumbo Grosso (TR-18S) (4)	1.816 ± 32 Ma	SHRIMP
	1.811 ± 44 Ma	$^{207}\text{Pb}/^{206}\text{Pb}$ -monazite
	1.807 ± 28 Ma	(hydrothermal alteration)

References: (1) Assis *et al.* (2012) and Assis (2015); (2) Moura (1998) Matupá Intrusive Suite; (3) Miguel Jr. (2011) Pé Quente Monzonite and União do Norte Porphyry; (4) this work; (5) Acevedo (2014).

Table 3. Description of samples from Trairão and Chumbo Grosso deposits. Minerals selected for SHRIMP II analyses.

Sample	Rock Type	Coordinates*	Age (Ma)	SiO ₂ (%wt)	Analyzed Mineral
TR-20T	Au-magnetite quartz breccia Hydrothermal rock	$09^{\circ}48'25''$ $55^{\circ}34'47''$	1798 ± 12 Ma Minimum age of ore formation	75%	monazite
TR-18S	Au-sulphides vein Hydrothermal rock	$09^{\circ}47'37''$ $55^{\circ}40'43''$	1805 ± 22 Ma Minimum age of ore formation	72%	monazite
TRBY-20	Biotite syenogranite Host rock	$09^{\circ}48'25''$ $55^{\circ}35'11''$	1854 ± 8 Ma Magmatic crystallization	76%	zircon
TRBY-27	Biotite syenogranite Host rock	$09^{\circ}50'03''$ $56^{\circ}20'23''$	1878 ± 8 Ma Magmatic crystallization	70%	zircon

*Coordinates are referenced to SAD 69 (South American Datum) zone 21 Southern Hemisphere.

associated with the later magmatism of Tapajos-Parimá Province (Jurueña Arc) responsible for remobilization and transport of gold enriched hydrothermal fluids, during the Statherian period. In this context, the present paper aims to contribute to a better understanding of the gold metallogenesis associated with the granite systems in AFGP through a comparative study between other gold deposits.

ARTICLE INFORMATION

Manuscript ID: 20190063. Received on: 08/12/2019. Approved on: 02/14/2020.

F. J.: Orientation of the development of research and review of geochronological data of the article, wrote the first draft of the manuscript. J. S.: Provided advisory regarding Amazon Craton geology, improved the manuscript through corrections and suggestions, made a comparison on the ages of other gold deposits in the region. M. B.: Provided data on the geology and geochronology of Alta Floresta Gold Province, revised and improved the manuscript. F. P.: Support in the pre-field stage (literature review of the study area) and in field activities. N. M.: Participation in laboratory activities with acquisition of mineral chemistry data in monazite. P. C.: Support in the pre-field stage (literature review of the study area) and in field activities. M. R.: Participation in the laboratory stages with acquisition and interpretation of geochronological data. Competing interests: The authors declare no competing interests.

REFERENCES

- Acevedo A.A. 2014. *The Jurueña Gold Deposit, Northwestern Sector of The Alta Floresta Province: an example of Paleoproterozoic gold-rich porphyry system?* Dissertation, Universidade Estadual de Campinas, Campinas, 58 p.
- Ague J.J. 2014. *Fluid Flow in the Deep Crust, Treatise on Geochemistry*. 2ª ed. Cidade, Elsevier, p. 203-247.
- Almeida F.F.M., Hasui Y., Brito Neves B.B., Fuck R.A. 1981. Brazilian structural provinces: an introduction. *Earth Sciences Review*, **17**:1-29. [https://doi.org/10.1016/0012-8252\(81\)90003-9](https://doi.org/10.1016/0012-8252(81)90003-9)
- Amaral G. 1974. *Geologia Pré-Cambriana da Região Amazônica*. Thesis, Universidade de São Paulo, São Paulo, 212 p.
- Assis R.R. 2015. *Depósitos auríferos associados ao magmatismo félsico da Província de Alta Floresta (MT), Cráton Amazônico: idade das mineralizações, geoquímica e fonte dos fluidos*. Thesis, Instituto de Geociências, Universidade Estadual de Campinas, 363 p.
- Assis R.R., Xavier R.P., Paes de Barros A.J., Barbuena D., Miguel-Jr E. 2012. Contexto geológico e litogeoquímica das unidades plutônicas-vulcânicas da região de União do Norte, setor leste da Província Aurífera de Alta Floresta (MT). *Revista Brasileira de Geociências*, **42**(1):130-161. <https://doi.org/10.25249/0375-7536.2012421130161>
- Barros M.A.S., Barros A.J.P., Santos J.O.S., Rocha M.L.B.P. 2015. Extension of The Tapajós Domains to The Alta Floresta Gold Province: Evidence From U-Pb SHRIMP Ages of the Nhandu Intrusive Suite At 1962 And 1967 Ma. In: *Simpósio de Geologia da Amazônia*, 14. *Anais...*
- Barros M.A.S., Chemale Jr. F., Nardi L.V.S., Lima E.F. 2009. Paleoproterozoic bimodal post-collisional magmatism in the southwestern Amazonian Craton, Mato Grosso, Brazil: geochemistry and isotopic evidence. *Journal of South American Earth Sciences*, **27**(1):11-23.
- Bettencourt J.S. et al. 2016. Metallogenic systems associated with granitoid magmatism in the Amazonian Craton: An overview of the present level of understanding and exploration significance. *Journal of South American Earth Sciences*. **68**:22-49.
- Braun I., Montel J.-M., Nicollet C. 1998. Electron microprobe dating of monazites from high-grade gneisses and pegmatites of the Kerala Khondalite Belt, southern India. *Chemical Geology*, **146**(1-2):65-85.
- Candela P.A. 1997. A review of shallow, ore-related granites: textures, volatiles, and metals. *Journal of Petrology*, **38**(12):1619-1633. <https://doi.org/10.1093/ptro/38.12.1619>
- Chang L.L.Y., Howie R.A., Zussman J. 1996. *Rock-forming minerals*. Harlow, Longman Group, 383 p. v. 5B.
- Cocherie E., Be Mezeme O., Legendre C.M., Fanning M., Faure, P. Rossi. 2005. Electron-microprobe dating as a tool for determining the closure of Th-U-Pb systems in migmatitic monazites. *American Mineralogist*, **90**:607-618.
- Compston W., Williams I.S., Campbell I.H., Gresham J.J. 1986. Zircon xenocrysts from the Kambalda volcanics: Age constraints and direct evidence for the older continental crust below the Kambalda-Norseman greenstones. *Earth and Planetary Science Letters*, **76**(3-4):299-311.
- Dardene M.A., Schobbenhaus C. 2001. *Metalogênese do Brasil*. Brasília, Ed. Universidade de Brasília, 392 p.
- Duarte T.B. 2015. *Geologia, Geoquímica e Geocronologia do Domínio Vulcânico do Arco Magmático Jurueña, SW do Cráton Amazônico: Implicações Geotectônicas*. Dissertação, Instituto de Geociências, Universidade Estadual de Campinas, Campinas.
- Fletcher I.R., McNaughton N.J., Davis W.J., Rasmussen B. 2010. Matrix effects and calibration limitations in ion probe U-Pb and Th-Pb dating of monazite. *Chemical Geology*, **270**(1-4):31-44. <https://doi.org/10.1016/j.chemgeo.2009.11.003>
- Förster H.J. 1998. The chemical composition of REE-Y-Th-U rich accessory minerals in peraluminous granite of the Erzgebirge-Fichtelgebirge region, Germany, Part I: the monazite - (Ce) - brabantite solid solution series. *American Mineralogist*, **83**(3-4):259-272. <https://doi.org/10.2138/am-1998-3-409>
- Foster G., Kinny P., Vance D., Prince C., Harris N. 2000. The significance of monazite U-Th-Pb age data in metamorphic assemblages; a combined study of monazite and garnet chronometry. *Earth Planetary Sciences Letters*, **181**(3):327-340. [https://doi.org/10.1016/S0012-821X\(00\)00212-0](https://doi.org/10.1016/S0012-821X(00)00212-0)
- Gonçalves G.O., Lana C., Buick I.S., Alkmim F.F., Scholz R., Queiroga G. 2019. Twenty million years of post-orogenic fluid production and hydrothermal mineralization across the external Araçuaí orogen and adjacent São Francisco Craton, SE Brazil. *Lithos*, **342-343**:557-572. <https://doi.org/10.1016/j.lithos.2019.04.022>
- Jaffey A.H., Flynn K.F., Glendenin L.E., Bentley W.C., Essling A.M. 1971. Precision measurement of half lives and specific activities of ²³⁵U and ²³⁸U. *Physics Reviews*, **4**:1889-1906. <https://doi.org/10.1103/PhysRevC.4.1889>
- Kucha H. 1980. Continuity in the monazite-hyuttonite series. *Mineralogical Magazine*, **43**:1031-1034.
- Lobato L.M., Santos J.O.S., McNaughton N.J., Fletcher I.R., Noce C.M. 2007. U-Pb SHRIMP monazite ages of the giant Morro Velho and Cuiabá gold deposits, Rio das Velhas greenstone belt, Quadrilátero Ferrífero, Minas Gerais, Brazil. *Ore Geology Reviews*, **32**(3-4):674-680. <https://doi.org/10.1016/j.oregeorev.2006.11.007>
- Ludwig K.R. 2001. *Using Isoplot/Ex. A geochronological toolkit for Microsoft Excel*. Special Publications No. 1. Berkeley, Berkeley Geochronology Center.

- Ludwig K.R. 2009. *SQUID 2: A User's Manual*, rev. 2.50. Special Publication 5. Berkeley, Berkeley Geochronology Centre, 110 p.
- Martins B.S., Lobato L.M., Rosière C.A., Hagemann S.G., Santos J.O.S., Villanova F.L.S.P., Silva R.C.F., Lemos L.H.A. 2016. The Archean BIF-hosted Lamego gold deposit, Rio das Velhas greenstone belt, Quadrilátero Ferrífero: Evidence for Cambrian structural modification of an Archean orogenic gold deposit. *Ore Geology Reviews*, **72**(Part 1):963-988. <https://doi.org/10.1016/j.oregeorev.2015.08.025>
- Miguel Jr. E. 2011. *Controle Estrutural das mineralizações auríferas e idades U-Pb das rochas encaixantes ao longo do Lineamento Peru-Trairão: Província Aurífera de Alta Floresta, Mato Grosso*. Dissertation, Instituto de Geociências, Universidade Estadual de Campinas, Campinas, 41 p.
- Montel J.M., Forest S., Veschambre M., Nicollet C., Provost A.A. 1996. Fast, reliable, inexpensive in-situ dating technique: electron microprobe ages on monazite. *Chemical Geology*.
- Moura M.A. 1998. O maço granítico Matupá no depósito de ouro Serrinha (MT): petrologia, alteração hidrometal e metalogenia. Tese de Doutorado, Instituto de Geociências, Universidade de Brasília. 238 p.
- Moura M.A., Botelho N.F. 2002. Petrologia do magmatismo associado à mineralização do tipo ouro pórfiro a província aurífera Juruena -Teles Pires (MT). *Revista Brasileira de Geociências*, **32**(3):377-386.
- Nakamura N. 1974. Determination of REE, Ba, Fe, Mg, Na and K in carbonaceous and ordinary chondrites. *Geochimica et Cosmochimica Acta*, **38**(5):757-775. [https://doi.org/10.1016/0016-7037\(74\)90149-5](https://doi.org/10.1016/0016-7037(74)90149-5)
- Paes de Barros A.J. 2007. *Granitos da região de Peixoto de Azevedo – Novo Mundo e mineralizações auríferas relacionadas – Província Aurífera Alta Floresta (MT)*. Tese, Instituto de Geociências, Universidade Estadual de Campinas, Campinas, 154 p.
- Parrish R.R. 1990. U-Pb dating of monazite and its application to geological problems. *Canadian Journal of Earth Sciences*, **27**(11):1431-1450. <https://doi.org/10.1139/e90-152>
- Paterson S.R., Ducea M.N. 2015. Arc Magmatic Tempos: Gathering the Evidence. *Elements*, **11**(2):91-98. <https://doi.org/10.2113/gselements.11.2.91>
- Pinho M.A.S., Chemale Jr. F., Schmus W.R.V., Pinho F.E.C. 2003. U–Pb and Sm–Nd evidence for 1.76–1.77 Ga magmatism in the Moriru region, Mato Grosso, Brazil: implications for province boundaries in the SW Amazonian Craton. *Precambrian Research*, **126**:1-25. [http://dx.doi.org/10.1016/S0301-9268\(03\)00126-8](http://dx.doi.org/10.1016/S0301-9268(03)00126-8)
- Poittrasson F., Chenery S., Shepherd T.J. 2000. Electron microprobe and LA-ICP-MS study of monazite hydrothermal alteration: implications for U-Th-Pb geochronology and nuclear ceramics. *Geochimica et Cosmochimica Acta*, **64**(19):3283-3297. [https://doi.org/10.1016/S0016-7037\(00\)00433-6](https://doi.org/10.1016/S0016-7037(00)00433-6)
- Rasmussen B., Fletcher I.R., Muhling J.R., Thorne W.S., Broadbent G.C. 2007. Prolonged history of episodic fluid flow in giant hematite ore bodies: Evidence from in situ U–Pb geochronology of hydrothermal xenotime. *Earth and Planetary Science Letters*, **258**(1-2):249-259. <https://doi.org/10.1016/j.epsl.2007.03.033>
- Rasmussen B., Fletcher I.R., McNaughton N.J. 2001. Dating low-grade metamorphism by SHRIMP U-Pb analysis of monazite in shales. *Geology*, **29**(10):963-966. [https://doi.org/10.1130/0091-7613\(2001\)029%3C0963:DLGMEB%3E2.0.CO;2](https://doi.org/10.1130/0091-7613(2001)029%3C0963:DLGMEB%3E2.0.CO;2)
- Rasmussen B., Sheppard S., Fletcher I.R. 2006. Testing ore deposit models using in situ U-Pb geochronology of hydrothermal monazite: Paleoproterozoic gold mineralization in northern Australia. *Geology*, **34**(2):77-80. <https://doi.org/10.1130/G22058.1>
- Rocha M.L.B.P. 2016. *Estudos geoquímicos e geocronológicos aplicados às rochas graníticas do garimpo Trairão - MT*. Thesis, Instituto de Geociência, Universidade de Brasília, Brasília, 136 p.
- Santos J.O.S. 2000. *Os terrenos Paleoproterozóicos da Província do Tapajós e as mineralizações de ouro associadas*. Thesis, Universidade Federal do Rio Grande do Sul, Porto Alegre, 208 p.
- Santos J.O.S. 2003. Geotectônica dos escudos das Guianas e Brasil-Central. In: Bizzi L.A., Schobbenhaus C., Vidotti R.M., Gonçalves J.H. (eds.), *Geologia, tectônica e recursos minerais do Brasil*. Brasília, CPRM. CD-ROM.
- Santos J.O.S., Rizzotto G.J., Chemale F., Hartmann L.A., Quadros M.L.E.S., McNaughton N.J. 2003. Three distinctive collisional orogenies in the southwestern Amazon Craton: Constraints from U-Pb geochronology. *South American Symposium on Isotope Geology*, **4**, Companhia Bahiana de Pesquisa Mineral, Salvador, Bahia, Short papers, 1:282-285.
- Santos J.O.S., Van Breemen O.B., Groves D.I., Hartmann L.A., Almeida M.E., McNaughton N.J., Fletcher I.R. 2004. Timing and evolution of multiple Paleoproterozoic magmatic arcs in the Tapajós Domain, Amazon Craton: constraints from SHRIMP and TIMS zircon, baddeleyite and titanite U-Pb geochronology. *Precambrian Research*, **131**(1-2):73-109. <https://doi.org/10.1016/j.precamres.2004.01.002>
- Serrato A.A.A. 2014. *Geocronologia e evolução do sistema hidrotermal do depósito aurífero de Juruena, Província Aurífera de Alta Floresta (MT), Brasil*. Dissertation, Universidade de Campinas, Campinas.
- Silva F.R., Barros M.A.S., Pierosan R., Pinho F.E.C., Rocha M.L.B.P., Vasconcelos B.R., Dezula S.E.M., Tavares C., Rocha J. 2014. Geoquímica e geocronologia U-Pb (SHRIMP) de granitos da região de Peixoto de Azevedo: Província Aurífera Alta Floresta, MT. *Brazilian Journal of Geology*, **44**(3):433-455. <https://doi.org/10.5327/Z2317-4889201400030007>
- Silva M.G., Abram M.B. 2008. *Projeto Metalogenia da Província Aurífera Juruena-Teles Pires, Mato Grosso*. Goiânia, Serviço Geológico Brasileiro, CPRM, 212 p.
- Smith J.B., Barley M.E., Groves D.I., Krapez B., McNaughton N.J., Bickle M.J., Chapman H.J. 1998. The Scholl shear zone, West Pilbara: Evidence for a domain boundary structure from integrated tectonostratigraphic analyses, SHRIMP U-Pb dating and isotopic and geochemical data of granitoids. *Precambrian Research*, **88**(1-4):143-171.
- Souza J.P., Frasca A.A.S., Oliveira C.C. 2005a. *Geologia e Recursos Minerais da Província Mineral de Alta Floresta. Relatório Integrado*. Brasília, Serviço Geológico Brasileiro (CPRM), 164 p.
- Souza V.S., Teixeira L.M., Botelho N.F. 2005b. Datação U-Th-Pb de Monazita Hidrotermal e sua aplicação na Geocronologia da Mineralização de Estanho em zonas de greisen do sistema Granítico Palanqueta, Depósito do Bom Futuro (RO). *Revista Brasileira de Geociências*, **35**(1):43-48.
- Tassinari C.C.G., Macambira M.J.B. 1999. Geochronological provinces of the Amazonian Craton. *Episodes*, **22**(3):173-182.
- Teufel S., Heinrich W. 1997. Partial resetting of the U-Pb isotope system in monazite through hydrothermal experiments: an SEM and U-Pb isotope study. *Chemical Geology*, **137**(3-4):273-281. [https://doi.org/10.1016/S0009-2541\(96\)00161-1](https://doi.org/10.1016/S0009-2541(96)00161-1)
- Williams I.S., Claesson S. 1987. Isotopic evidence for the Precambrian provenance and Caledonian metamorphism of high grade paragneisses from the Steve Nappes, Scandinavian Caledonides, II. Ion microprobe zircon U-Th-Pb. *Contributions to Mineralogy and Petrology*, **97**:205-217.
- Xavier R.P., Assis R.R., Creaser R., Trevisan G.V., Paes de Barros A.J., Acevedo A., Miguel-Junior E., Barros M.S.A., Pinho F.E.C. 2013. Timing of gold metallogeny in the Alta Floresta Gold Province: Evidence from pyrite and molybdenite Re-Os isotopic dating. In: Congresso de Geologia da Amazônia, 13., Belém. *Anais...* 4 p.
- Yardley B.W.D. 2009. The role of water in the evolution of the continental crust. *Journal of Geological Society*, **166**(4):585-600. <https://doi.org/10.1144/0016-76492008-101>